PCP
PLANT & CELL PHYSIOLOGY

BES1 and BZR1 Redundantly Promote Phloem and Xylem Differentiation

Masato Saito*, Yuki Kondo and Hiroo Fukuda*

Department of Biological Sciences, Graduate School of Science, The University of Tokyo, 7-3-1 Hongo, Bunkyo-ku, Tokyo, 113-0033 Japan
*Corresponding authors: Masato Saito, E-mail, msaito@bs.s.u-tokyo.ac.jp; Fax, +81-3-5841-4462; Hiroo Fukuda, E-mail, fukuda@bs.s.u-tokyo.ac.jp; Fax, +81-3-5841-4462.
(Received October 2, 2017; Accepted January 14, 2018)

Regular Paper

Vascular development is a good model for studying cell differentiation in plants. Two conductive tissues, the xylem and phloem, are derived from common stem cells known as procambial/cambial cells. Glycogen synthase kinase 3 proteins (GSK3s) play crucial roles in maintaining procambial/cambial cells by suppressing their differentiation into xylem or phloem cells. We previously designed an *in vitro* culture system for analyzing vascular cell differentiation named VISUAL (Vascular cell Induction culture System Using Arabidopsis Leaves). Using this system, we found that the transcription factor BRI1-EMS-SUPPRESSOR 1 (BES1) functions as a downstream target of GSK3s during xylem differentiation. However, the function of BES1 in vascular development remains largely unknown. Here, we found that, in addition to xylem differentiation, BES1 positively regulates phloem differentiation downstream of GSK3s. Transcriptome analysis using VISUAL confirmed that BES1 promotes bi-directional differentiation of procambial cells into xylem and phloem cells. Genetic analysis of loss-of-function mutants newly generated using the CRISPR/Cas9 (clustered regularly interspaced short palindromic repeats/CRISPR-associated protein 9) system revealed that BRASSINAZOLE RESISTANT 1 (BZR1), the closest homolog of BES1, functions in vascular development redundantly with BES1. Notably, BZR1 has a weaker impact on vascular cell differentiation than BES1, suggesting that they contribute differentially to this process. In conclusion, our findings indicate that BES1 and BZR1 are key regulators of both xylem and phloem cell differentiation from vascular stem cells.

Keywords: Arabidopsis • BES1 • CRISPR/Cas9 • Phloem • Vascular development • VISUAL.

Abbreviations: APL, ALTERED PHLOEM DEVELOPMENT; ARF, AUXIN RESPONSE FACTOR; ARR, ARABIDOPSIS RESPONSE REGULATOR; BEH, BES1/BZR1 HOMOLOG; BES1, BRI1-EMS-SUPPRESSOR 1; BL, brassinolide; BR, brassinosteroid; BRI1, BRASSINOSTEROID-INSENSITIVE 1; BZR1, BRASSINAZOLE RESISTANT 1; CRISPR, clustered regularly interspaced short palindromic repeats; Cas9, CRISPR-associated protein 9; DMSO, dimethylsulfoxide; GO, Gene Ontology; GSK3, glycogen synthase kinase 3 protein; IRX3, IRREGULAR XYLEM 3; MS, Murashige and Skoog; PAM, protospacer adjacent motif; qRT-PCR, quantitative reverse transcription PCR; SEOR1, SIEVE-ELEMENT-OCCLUSION-RELATED 1; sgRNA, single guide RNA; TDR, TDIF RECEPTOR; UBQ14, UBIQUITIN 14; VISUAL, Vascular cell Induction culture System Using Arabidopsis Leaves; VND, VASCULAR-RELATED NAC-DOMAIN; VP, VISUAL phloem-specific gene; WT, wild type; XCP1, XYLEM CYSTEINE PEPTIDASE 1.

Footnote: Microarray data have been deposited in Gene Expression Omnibus (https://www.ncbi.nlm.nih.gov/geo/). Accession number is GSE110199.

Introduction

Vascular tissues, comprising xylem and phloem cells, are required for long-distance transport of various materials in plants. The xylem transports water and minerals from roots to shoots, whereas, in most cases, the phloem transports photoassimilates from shoots to roots. Although xylem and phloem cells have different structures and functions, these cells originate from common stem cells known as procambial/cambial cells. Previous studies identified master regulators of xylem and phloem cell fate. VASCULAR-RELATED NAC-DOMAINs (VNDs) facilitate xylem differentiation (Kubo et al. 2005), whereas ALTERED PHLOEM DEVELOPMENT (APL) is required for phloem development (Bonke et al. 2003). Molecular analyses of these master regulators have revealed the downstream components controlling various developmental events associated with xylem and phloem differentiation (Ohashi-Ito et al. 2010, Yamaguchi et al. 2011, Furuta et al. 2014b). Prior to the final determination of cell fate, glycogen synthase kinase 3 proteins (GSK3s) regulate vascular cell differentiation as earlier regulators (Kondo et al. 2014). The SKI and SKII subgroups of GSK3s redundantly maintain procambial cell populations by suppressing xylem differentiation. Indeed, the application of the GSK3 inhibitor bikinin (De Rybel et al. 2009) induces ectopic xylem cell differentiation in the presence of auxin and cytokinin (Kondo et al. 2014, Kondo et al. 2015). This feature allowed us to establish a powerful tissue culture system for vascular cell differentiation named VISUAL (Vascular cell Induction culture System Using Arabidopsis Leaves). Using VISUAL, we found that ectopic xylem differentiation induced by the inhibition of GSK3s is suppressed in mutants for BRI1-EMS-SUPPRESSOR 1 (BES1) (Kondo et al. 2014, Kondo et al. 2015), a direct substrate of GSK3s (Yin et al. 2002). Bikinin also has a promotive effect on phloem differentiation in VISUAL (Kondo et al. 2016). However, it remains

Plant Cell Physiol. 59(3): 590–600 (2018) doi:10.1093/pcp/pcy012, Advance Access publication on 27 January 2018, available online at www.pcp.oxfordjournals.org

to be elucidated whether BES1 regulates phloem differentiation downstream of GSK3s and, if so, how BES1 regulates both phloem and xylem differentiation.

The GSK3s–BES1 signaling module is also involved in the brassinosteroid (BR) signaling pathway. The perception of BR by BRASSINOSTEROID-INSENSITIVE 1 (BRI1) leads to the inactivation of GSK3s (Li and Nam 2002). BES1 family transcription factors are then activated to control downstream gene expression (Yin et al. 2005). Arabidopsis contains six members of the BES1 family. Among these, BES1 and its closest homolog, BRASSINAZOLE RESISTANT 1 (BZR1), are considered to be major mediators of BR signaling. However, our understanding of the BR signaling pathway has primarily been obtained from studies using the gain-of-function mutants *bes1-D* and *bzr1-D* (Yin et al. 2002, Wang et al. 2002). In contrast, few loss-of-function studies investigating BES1 family members have been performed (Yin et al. 2005). In particular, loss-of-function mutants for *BZR1* have not yet been reported. Therefore, our understanding of the contribution of BES1 and BZR1 to BR signaling remains incomplete. As for vascular development, we also analyzed the role of BES1 and BZR1 using gain-of-function mutants (Kondo et al. 2014). However, recent advances in genome editing techniques, including the CRISPR/Cas9 (clustered regularly interspaced short palindromic repeats/CRISPR-associated protein 9) system, should allow the actual functions of genes of interest to be analyzed by generating knock-out mutants.

In this study, we investigated the functions of BES1 and BZR1 in vascular cell differentiation using loss-of-function mutants generated via the CRISPR/Cas9 system. Comprehensive gene expression analysis of the *bes1* mutants revealed that BES1 positively regulates both xylem and phloem differentiation, but not procambial cell differentiation from mesophyll cells, in VISUAL. Further genetic analysis with *bes1 bzr1* mutants indicated that BES1 and BZR1 act redundantly in promoting both xylem and phloem differentiation. Interestingly, the phenotypes when cultured in VISUAL were weaker in *bzr1* than in *bes1*, indicating that BES1 and BZR1 contribute differently to vascular development. Consistently, *bes1 bzr1* plants displayed lower sensitivity to exogenous BR treatment than the *bes1* single mutants but were still sensitive to BR, suggesting the further functional redundancy of BES1 family members.

Results

BES1 positively regulates xylem cell differentiation in VISUAL

We previously found that *bes1* mutants have defects in xylem differentiation when cultured in VISUAL (Kondo et al. 2014, Kondo et al. 2015). To investigate further the role of BES1 in vascular development, we obtained three T-DNA insertion lines for *BES1*: *bes1-1* (He et al. 2005), *bes1-2* (Lachowiec et al. 2013) and *bes1-3* (previously named *bes1-2* in Kang et al. 2015, and *bes1* in Kondo et al. 2014) (**Fig. 1A**). None of the mutants showed visible phenotypes in terms of plant growth and xylem development in vivo. However, the cotyledons of these mutants commonly exhibited reduced xylem differentiation at 96 h after VISUAL induction (**Fig. 1B–E**). Differentiation rates in *bes1-1* and *bes1-2* mutants were lower than that in *bes1-3*, indicating that *bes1-1* and *bes1-2* are strong alleles and that *bes1-3* is a weak allele. We performed detailed phenotypic analysis of *bes1-3* (weak allele) and *bes1-1* (strong allele) by monitoring the expression of vascular marker genes. RNA samples were collected at 72 h after induction, when xylem-related genes were expressed at maximum levels. Our quantitative reverse transcription PCR (qRT-PCR) analysis indicated that the expression levels of xylem marker genes such as *IRREGULAR XYLEM 3* (*IRX3*) and *XYLEM CYSTEINE PEPTIDASE 1* (*XCP1*) were lower in the *bes1* mutants than in the wild type (WT) and were lower in *bes1-1* than in *bes1-3* (**Fig. 2A, B**). Next, we introduced a genomic fragment of *BES1* (*gBES1*) into *bes1-1*. The introduction completely restored the reduced ectopic xylem differentiation rate and xylem-related gene expression in *bes1-1* (**Fig. 3**). These results further support the notion that BES1 positively regulates xylem differentiation.

BES1 promotes xylem cell differentiation from procambial cells in VISUAL

In VISUAL, mesophyll cells first differentiate into procambial cells, followed by xylem cells (Kondo et al. 2015). We therefore examined whether *BES1* is involved in the induction of procambial cells, xylem differentiation from procambial cells or both processes. First, we used the procambium-specific gene *TDIF RECEPTOR* (*TDR*) as a marker and found that this gene was not down-regulated in *bes1* mutants in VISUAL. Next, to dissect downstream and upstream factors for BES1 comprehensively, we performed microarray analysis of cotyledons at 72 h after VISUAL induction in *bes1-1*, *bes1-3* and the WT. We initially selected genes that were highly up-regulated at 72 h after VISUAL induction in the WT (>4-fold up-regulation, 1,534 genes; Kondo et al. 2016) as vascular-related genes. Hierarchical clustering classified the vascular-related genes into two major groups. Approximately 60% of the vascular-related genes were down-regulated in *bes1* mutants. Then we designated these genes as a '*bes1*-down' group (**Fig. 2F**). On the other hand, nearly 40% of vascular-related genes were expressed at the same or a higher level in the mutants. Therefore, we categorized these genes as a '*bes1*-not-down' group (**Fig. 2F**). To characterize these two groups of genes, we analyzed the expression profiles of the *bes1*-down group and the *bes1*-not-down group using our previously reported time course microarray data from leaf disks cultured in VISUAL (Kondo et al. 2015). Most *bes1*-down genes were highly expressed 60 h after induction, whereas many *bes1*-not-down genes were induced 36 h after induction (**Fig. 2G**). This analysis indicated that the *bes1*-not-down and the *bes1*-down genes begin to be expressed at early and late stages in VISUAL, respectively. Further half-time point analysis, which evaluates the timing of gene expression in VISUAL, indicated that the expression of the *bes1*-not-down genes increased from 12 to 26 h and that of the *bes1*-down genes increased from 30 to 48 h in VISUAL (**Fig. 2H**). These results indicate that, in the *bes1* mutants, the late stage of VISUAL is suppressed, whereas the early stage is not suppressed but is instead promoted.

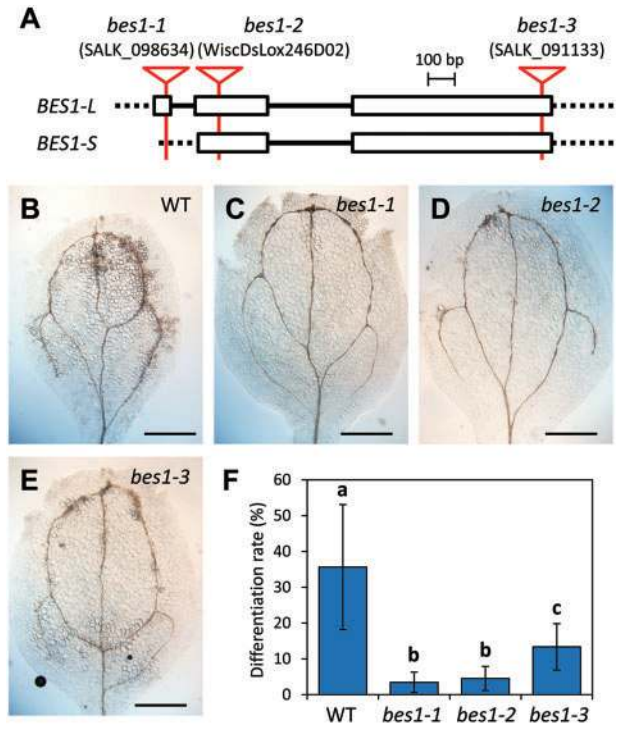

Fig. 1 Phenotypes of *bes1* T-DNA insertion mutants in VISUAL. (A) Schematic diagram of the exon–intron structures of *BES1*. Two splicing variants (Jiang et al. 2015) are shown. Exons, introns and untranslated regions are illustrated by boxes, black solid lines and dotted lines, respectively. Red lines represent putative insertion sites of T-DNA in each *bes1* mutant. (B–E) Ectopic xylem cell formation in VISUAL. WT (B), *bes1-1* (SALK_098634) (C), *bes1-2* (WiscDsLox246D02) (D) and *bes1-3* (SALK_091133) (E) cotyledons were cultured in medium containing 2,4-D, kinetin and bikinin for 4 d. Scale bars indicate 1 mm. (F) Quantification of xylem differentiation rates in (B–E). Error bars indicate the SD (n = 8–10). Significant differences are indicated by different letters (Tamhane T2 test, α = 0.05).

We then conducted Gene Ontology (GO) enrichment analysis to characterize the molecular functions of the *bes1*-down and *bes1*-not-down genes. In the *bes1*-down group, secondary cell wall-related genes, including xylan and lignin biosynthesis genes, were markedly enriched (**Table 1**). Additionally, genes related to xylem vessel cell differentiation were also enriched in this group (**Table 1**). These results coincide with the finding that *bes1* mutants show defects in xylem differentiation in VISUAL. On the other hand, procambial cell-related genes were enriched in the *bes1*-not-down group (**Table 1**). Moreover, the *bes1*-not-down group includes many cell cycle and cell division genes (**Table 1**), including seven out of eight procambial-specific genes that were up-regulated in VISUAL only in the presence of bikinin (Kondo et al. 2015). Additionally, some *bes1*-not-down genes were annotated as auxin-related genes, which seem to be implicated in procambium formation in leaves (Furuta et al. 2014a). These results suggest that, in cultured *bes1* cotyledons, procambial cells accumulate due to the inhibition of differentiation of procambial cells into xylem cells. Altogether, these data support our hypothesis that BES1 promotes xylem cell differentiation from procambial cells in VISUAL.

BES1 also promotes phloem cell differentiation in VISUAL

In the WT, the differentiation of phloem sieve element-like cells also occurs in VISUAL (Kondo et al. 2016). Interestingly, several *bes1*-down genes were annotated as being related to phloem development (**Table 1**). Consistent with this notion, qRT-PCR analysis indicated that the expression levels of phloem marker genes *APL* and *SIEVE-ELEMENT-OCCLUSION-RELATED 1* (*SEOR1*) were significantly reduced in the *bes1* mutants compared with the WT, similar to xylem marker genes (**Fig. 2D, E**). These results suggest that phloem differentiation is also inhibited in *bes1*.

To understand the role of BES1 in phloem development, we investigated the expression of VISUAL phloem-specific genes (VPs), which we previously identified by transcriptome analysis (Kondo et al. 2016), using the *bes1* microarray data. Many VPs were down-regulated in the *bes1* mutants (**Fig. 2I**). These down-regulated genes were also down-regulated in the *apl* mutants (**Fig. 2J**), which have strong defects in phloem development in VISUAL (Kondo et al. 2016). Considering the significant reduction in *APL* expression in *bes1-1* (**Fig. 2D**), these data suggest that BES1 up-regulates a wide range of phloem sieve element-related genes, probably upstream of APL. In addition to the recovery of xylem differentiation, the decrease in expression of phloem genes in *bes1-1* was fully complemented by the introduction of *gBES1* (**Fig. 3**). These results strongly support the idea that BES1 promotes phloem differentiation as well as xylem differentiation (**Fig. 2K**).

BZR1 acts redundantly with BES1 in vascular development

In *bes1* mutants, the induction of both xylem and phloem marker genes in VISUAL was not completely repressed, suggesting that other factors may contribute to the promotion of the differentiation process. BZR1 is the closest homolog of BES1, with 88% identity (Wang et al. 2002). We therefore employed genome editing techniques (Fauser et al. 2014) in Col-0 and *bes1-1* to generate *bzr1-1* and *bes1-1 bzr1-2* plants, respectively. We succeeded in obtaining these homozygous lines, in which the *Cas9* gene had been removed. The *bzr1-1* mutant possesses a one base insertion in the second exon of *BZR1*, resulting in the appearance of a premature stop codon due to a frameshift (**Fig. 4A, C**). On the other hand, the *bes1-1 bzr1-2* double mutant has lost 29 bases of *BZR1* spanning from the 3′ end of the intron to the start of the second exon (**Fig. 4A**). Sequencing of *BZR1* transcripts revealed that the splicing site between the intron and the second exon is altered in *bes1-1 bzr1-2* (**Fig. 4B**), leading to a premature stop codon due to a frameshift (**Fig. 4C**).

We then investigated whether BZR1 functions in vascular development using VISUAL. The *bzr1-1* single mutants showed slightly reduced xylem differentiation rates (**Fig. 5A–D**). Further gene expression analysis revealed that xylem marker genes were slightly repressed in *bzr1-1* compared with the WT (**Fig. 5E**). The expression levels of phloem marker genes were not significantly different from those of the WT (P = 0.136 for *APL* and P = 0.036 for *SEOR1*), but they tended to be reduced in *bzr1-1*

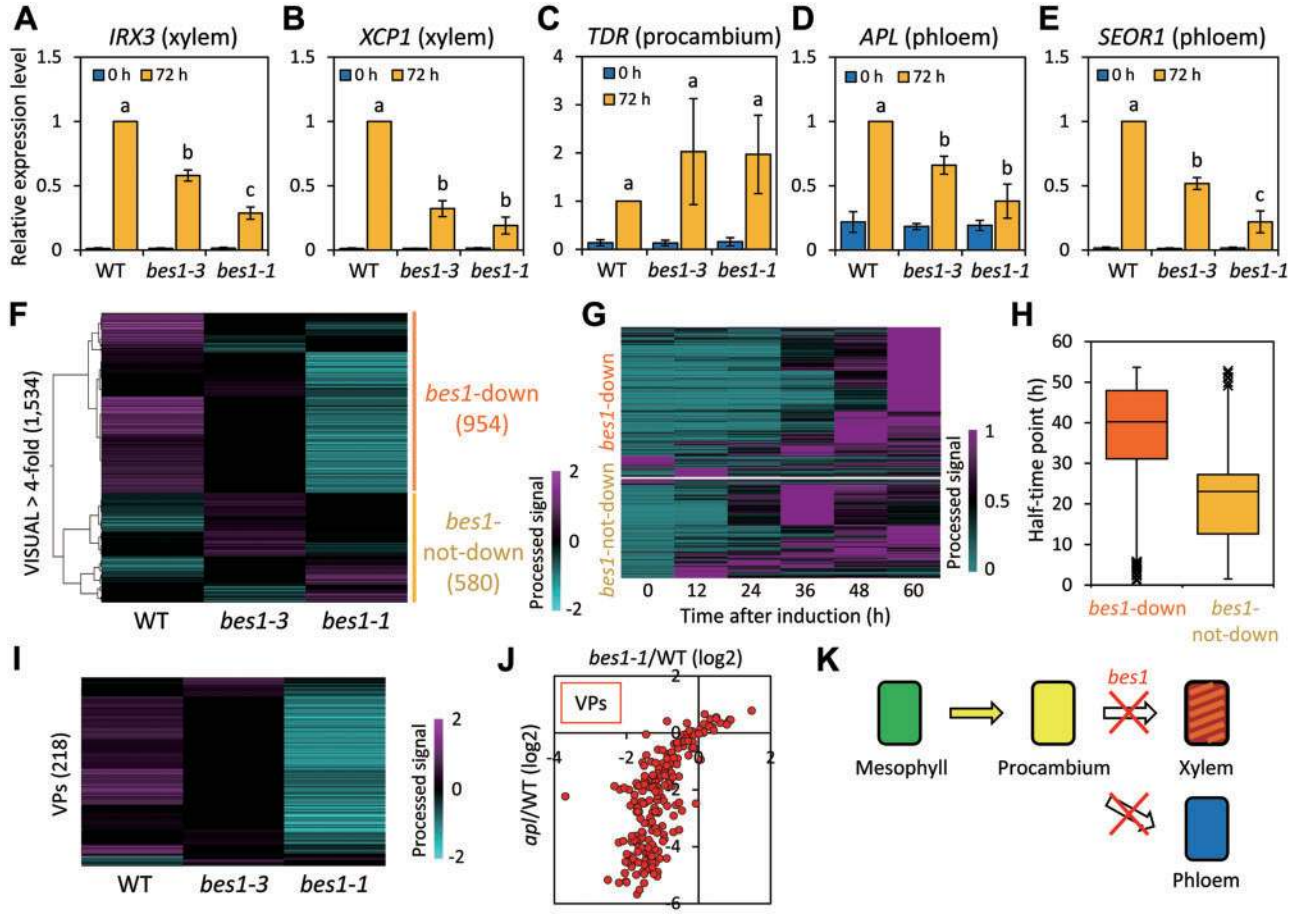

Fig. 2 Gene expression analysis of *bes1* mutants in VISUAL. (A–E) Expression levels of vascular-related marker genes in VISUAL. *IRX3* (A) and *XCP1* (B) are xylem-specific markers, *TDR* (C) is a procambium marker and *APL* (D) and *SEOR1* (E) are phloem markers. Relative expression levels were calculated by comparison with gene expression levels at 72 h in the WT. Error bars indicate the SD (n = 3). Significant differences among samples after induction are indicated by different letters (Tamhane T2 test, α = 0.05). (F) Hierarchical clustering of vascular-related genes. Each gene expression level was normalized by setting the median value of the WT, *bes1-3* and *bes1-1* as 0 (see the Materials and Methods). Two major clades were defined as the *bes1*-down and *bes1*-not-down group based on their expression pattern. Relative gene expression levels are visualized in a heatmap image according to the color scale shown in the right-hand panel. (G) Comparison of the time course of expression patterns between the *bes1*-down and *bes1*-not-down group. Each gene expression level was normalized by dividing the level by its maximum. (H) Box plot showing the distribution of the half-time point for each gene. The half-time point is defined as the first time point when the relative expression level reached 50% of its maximum. (I) Comparison of the expression patterns of VISUAL phloem-specific genes (VPs; Kondo etal. 2016). Expression levels are visualized in a heatmap image according to the color scale shown in the right-hand panel. (J) Comparison of the expression patterns of VPs in the WT vs. *bes1-1* and the WT vs. *apl* (Kondo etal. 2016) in VISUAL. The horizontal axis and vertical axis represent fold change in *bes1-1* and *apl* against the WT at the $\log_2$ scale, respectively. (K) Schematic illustration of the *bes1* mutant phenotype in VISUAL. The *bes1* mutations repress xylem and phloem differentiation from procambial cells.

(**Fig. 5E**). Thus, the mutant phenotypes of *bzr1-1* were weaker than those of *bes1-1* in terms of differentiation rate and gene expression level when cultured in VISUAL (**Fig. 5**). These results suggest that BZR1 is also involved in xylem and phloem differentiation, but to a lesser extent than BES1. We then investigated the relationship between the roles of BES1 and BZR1 in vascular cell differentiation using *bes1-1 bzr1-2* double mutants. However, the *bes1-1* mutants produced relatively small amounts of xylem cells under the original VISUAL conditions, preventing us from verifying the functional redundancy of *BES1* and *BZR1*. In an effort to solve this problem, we increased the bikinin concentration in the culture medium to 20 μM, because this treatment induced the production of more ectopic xylem cells in *bes1-1* than the original medium (**Fig. 6A, B**). Under this condition, the xylem differentiation rate was much lower in the *bes1-1 bzr1-2* mutants than in *bes1-1* (**Fig. 6C, D**). The down-regulation of xylem and phloem marker genes in the *bes1* single mutants was also enhanced by the addition of the *bzr1-2* mutation (**Fig. 6E**). On the other hand, the procambium marker gene *TDR* was not repressed in these mutants, even in *bes1-1 bzr1-2* (**Fig. 6E**). Based on these results, it is likely that BZR1 acts redundantly with BES1 in xylem and phloem differentiation from procambial cells in VISUAL.

Growth defects are not observed in bes1-1 bzr1-2 mutants

To investigate the functions of BES1 and BZR1 in in vivo vascular development, we compared cross-sections from WT vs.

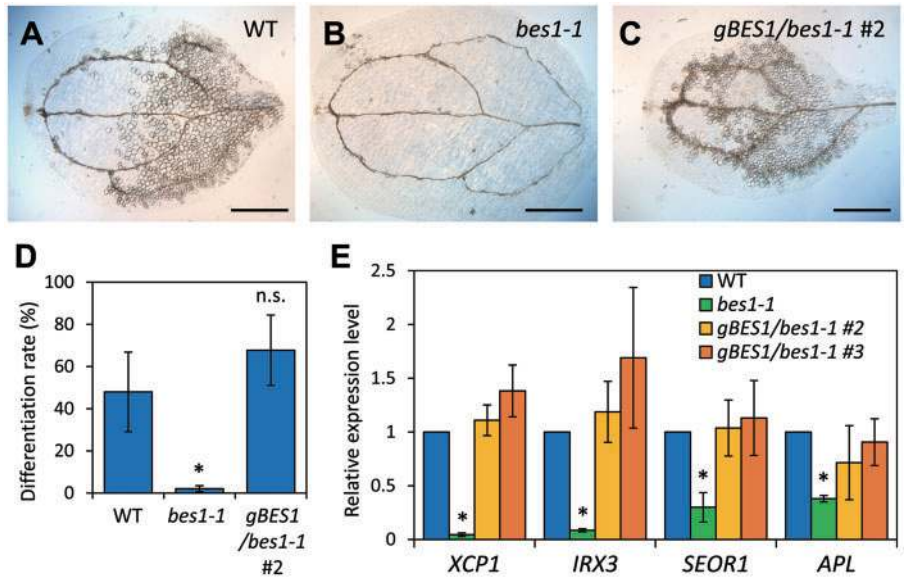

Fig. 3 Complementation test. (A–C) Ectopic xylem cell formation in VISUAL. Cotyledons of the WT (A), *bes1-1* (B) and *bes1-1* harboring genomic *BES1* (*gBES1/bes1-1*) (C) were cultured for 4 d. Scale bars indicate 1 mm. (D) Quantification of xylem differentiation rates in (A–C). Error bars indicate the SD (n = 8). Significant differences compared with the WT were examined by Tamhane T2 test (α = 0.05). (E) Expression levels of xylem and phloem marker genes in VISUAL. RNA was extracted from cotyledons at 72 h after VISUAL induction. Two independent complement lines were examined. Relative expression levels were calculated by comparison with the WT. Error bars indicate the SD (n = 3). Significant differences compared with the WT were examined by Tamhane T2 test (α = 0.05).

bes1-1 bzr1-2 plants. Although *bes1-1 bzr1-2* mutants showed severe defects in VISUAL, no obvious defects were observed in the central xylem tissues of hypocotyls in 16-day-old or 6-week-old plants (**Fig. 7A–D**). Phloem tissues (visualized by toluidine blue and aniline blue staining) were also indistinguishable between the WT and *bes1-1 bzr1-2* (**Fig. 7A–D**). Similarly, no defects in vascular development were observed in 6-week-old stems of *bes1-1 bzr1-2* (**Fig. 7E, F**). These results suggest that the vascular phenotype of *bes1-1 bzr1-2* is enhanced in the culture system VISUAL, in which exogenous bikinin induces rapid vascular cell differentiation apart from other developmental processes.

BES1 and BZR1 are involved in various developmental processes. In particular, they function as major transcription factors that mediate the BR signaling pathway (Guo et al. 2013). To explore the impact of BES1 and BZR1 on BR signaling, we treated WT and *bes1-1 bzr1-2* plants with brassinolide (BL). BL treatment promotes hypocotyl elongation and represses root growth in WT plants in the light. As previously reported (He et al. 2005, Kang et al. 2015), *bes1-1* was slightly resistant to exogenous BL (**Fig. 7G, H**). Although *bzr1-1* single mutants were partially resistant to exogenous BL only in root elongation, the *bes1-1 bzr1-2* mutants were more insensitive to BL than the *bes1* single mutants in terms of both hypocotyl and root elongation (**Fig. 7G, H**). Consistent with this observation, the changes in expression of a BR-responsive gene in response to BL treatment were also partially reduced in *bes1-1 bzr1-2* (**Supplementary Fig. S1**). Next, we investigated the defects related to BR signaling in *bes1-1 bzr1-2* in the absence of exogenous BL treatment. The *bri1* mutant, a BR receptor mutant, shows severe defects in hypocotyl elongation under dark conditions (Li and Chory 1997). However, *bes1-1* and *bes1-1 bzr1-2* did not exhibit this phenotype, instead appearing like WT plants (**Fig. 7I, J**). Furthermore, stem growth in *bes1-1 bzr1-2* was comparable with that in the WT under normal growth conditions, unlike the dwarf mutant *bri1* (**Supplementary Fig. S2**). These results indicate that the BR-related phenotype in *bes1-1 bzr1-2* appears only in the presence of exogenously applied BL.

BES1 and BZR1 gain-of-function mutations promote phloem differentiation in vivo

In contrast to *bes1-1 bzr1-2* mutants, it is known that gain-of-function mutants *bes1-D* and *bzr1-D* exhibit pleiotropic phenotypes. For instance, hypocotyl elongation is promoted in these mutants under darkness (Li and Nam 2002, Yin et al. 2002). Moreover, it was reported that the gain-of-function mutant *bes1-D* sometimes exhibits reduced procambial cell layers between xylem and phloem cells due to the excess vascular differentiation from procambial cells (Kondo et al. 2014). Then we generated *bes1-D bzr1-D* double gain-of-function mutants and observed their vascular phenotype in detail (**Fig. 8**). The overall morphology of *bes1-D bzr1-D* was similar to that of *bes1-D*, in which the hypocotyl is elongated (Yin et al. 2002), but the thickness of the hypocotyl is comparable with that of the WT. In WT hypocotyls, usually two or three procambial cell layers were formed between phloem and xylem cells (**Fig. 8A**). In *bes1-D bzr1-D*, however, procambial cell layers were reduced, occasionally resulting in adjacency of xylem and phloem cells (**Fig. 8B**; red arrowhead), which is consistent with the result in *bes1-D* (Kondo et al. 2014). In addition, ectopic phloem cells, which are non-clustered phloem cells

Table 1 GO enrichment analysis of vascular-related genes

Term	*P*-value	Fold enrichment
***bes1*-down genes**		
Regulation of secondary cell wall biogenesis	2.07E-15	24.88
Plant-type secondary cell wall biogenesis	1.29E-14	12.53
Xylan biosynthetic process	5.44E-13	15.88
Carbohydrate metabolic process	2.06E-07	2.75
Glucuronoxylan biosynthetic process	9.15E-07	17.87
Xylem development	1.56E-06	10.21
Xylan metabolic process	4.09E-06	20.42
Cell wall organization	4.79E-06	2.731
Lignin catabolic process	1.55E-05	11.91
Lignin biosynthetic process	6.65E-05	4.954
Xylem vessel member cell differentiation	7.05E-05	19.14
Cell wall thickening	1.35E-04	30.63
Phloem development	6.40E-04	20.42
Positive regulation of secondary cell wall biogenesis	6.40E-04	20.42
***bes1*-not-down genes**		
Microtubule-based movement	2.19E-19	15.32
Cell division	1.16E-14	6.134
Response to auxin	3.22E-12	4.77
Auxin-activated signaling pathway	3.10E-10	5.40
Cell cycle	1.40E-08	6.211
Mitotic nuclear division	4.34E-08	7.429
Regulation of cell cycle	1.15E-07	7.625
Multicellular organism development	6.54E-06	2.902
Procambium histogenesis	2.85E-05	24.76
Auxin polar transport	2.41E-04	6.368
Cotyledon vascular tissue pattern formation	5.90E-04	12.38

GO enrichment analysis of genes up-regulated in VISUAL (>4-fold, 1,534 genes). The *bes1*-down and *bes1*-not-down groups were examined separately. Significantly enriched terms ($P < 0.001$) are shown.

surrounded by undifferentiated cells, were sometimes formed only in *bes1-D bzr1-D* but not in the WT (**Fig. 8A, C**; yellow arrowhead). These results suggest that BES1 and BZR1 promote phloem differentiation from procambial cells in vivo.

Discussion

BES1 promotes xylem and phloem differentiation from procambial cells but not procambial cell differentiation from mesophyll cells

In a previous paper, we reported that BES1 promotes xylem differentiation from mesophyll cells in VISUAL (Kondo et al. 2014). In the current study, microarray analysis of *bes1* showed that BES1 promotes xylem differentiation from procambial cells but not procambial cell differentiation from mesophyll cells. We also found that the *bes1* mutations suppressed phloem differentiation in VISUAL, suggesting that BES1 plays a positive role in phloem differentiation. Microarray analysis also indicated that BES1 and APL share downstream genes involved in phloem differentiation. The expression of *APL* was repressed in *bes1*. These results indicate that BES1 positively regulates phloem differentiation, probably upstream of APL. On the other hand, the transcription factor genes *VND6* and *VND7*, encoding master regulators of xylem differentiation (Kubo et al. 2005), were also down-regulated in *bes1* (**Supplementary Table S1**). Therefore, it is likely that BES1 functions early in vascular development before the induction of final differentiation by master regulators of xylem and phloem differentiation. These findings, together with the observation that a large number of procambial cells remained in the *bes1* mutants after the induction of VISUAL, suggest that BES1 triggers the transition of stem cells to specialized cells into xylem or phloem cells.

Functional redundancy among BES1 family members

There are six *BES1*-like genes in the Arabidopsis genome: *BES1*, *BZR1* and *BES1/BZR1 HOMOLOG 1–4* (*BEH1–BEH4*) (Yin et al. 2002, Wang et al. 2002, Yin et al. 2005). BES1 and BZR1 are thought to act as central players that regulate various developmental processes in plants, playing prominent roles in BR signaling (Guo et al. 2013). However, in many cases, functional analyses of these proteins have been performed using gain-of-function mutants (*bes1-D* and *bzr1-D*), and few analyses have been performed using loss-of-function mutants. Here, we produced *bzr1-1* (a loss-of-function mutant of *BZR1*) and the *bes1-1 bzr1-2* double mutant to analyze the roles of BES1 and BZR1. The *bes1*, *bzr1-1* and *bes1-1 bzr1-2* mutants did not show any visible phenotypes in planta, including a dwarf phenotype and photomorphogenesis in the dark, which are characteristic phenotypes of BR-deficient mutants such as *bri1*. This result strongly suggests that BES1 family members function redundantly. We then examined the phenotypes of these mutants in physiological aspects. The only mutant phenotype observed in *bes1-1 bzr1-2* was reduced sensitivity to exogenous BL application. To account for this phenomenon, the following findings about other multiple mutants should be considered. The *arabidopsis response regulator 10* (*arr10*) *arr12* double mutants are resistant to exogenous cytokinin but grow well on Murashige and Skoog (MS) agar plates and in soil (Yokoyama et al. 2007). The addition of the *arr1* mutation to *arr10 arr12* results in plants with a dwarf phenotype in the absence of cytokinin, which was also observed in another cytokinin dominant-negative mutant, *wooden leg* (Yokoyama et al. 2007). Consistent with this idea, *bes1*-RNAi (RNA interference) lines, which exhibit repressed expression not only of *BES1* and *BZR1* (Yin et al. 2005), but also of several *BEH* genes (Wang et al. 2013), show defects in stem growth and shoot branching. Our results obtained using loss-of-function mutants raise the possibility that BEHs function redundantly with BES and BZR1. Further genetic analysis is needed to understand fully the functions of BES1 family proteins.

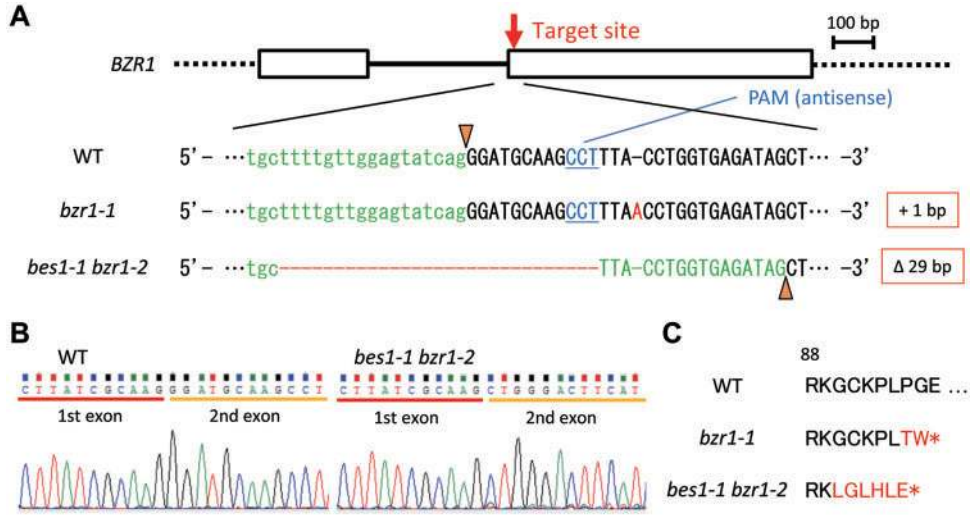

Fig. 4 Generation of *bzr1* mutants. (A) Schematic overview of the gene structure of *BZR1* and the sequence around the selected site targeted by CRISPR/Cas9. Exons, the intron and untranslated regions are illustrated by boxes, a solid line and dotted lines, respectively. Exon and intron sequences in the WT are written in lower case and upper case letters, respectively. The protospacer adjacent motif (PAM) sequences of the target and the resulting mutations are highlighted in blue and red, respectively. A one base insertion was detected in *bzr1-1*, whereas 29 base deletions occurred in *bes1-1 bzr1-2*. (B) The mRNA sequences of *BZR1* in the WT and *bes1-1 bzr1-2*. The splice site in each line is marked by an arrowhead, and spliced sequences are highlighted in green in (A). (C) Theoretical amino acid sequences of BZR1 around the mutated sites in the WT, *bzr1-1* and *bes1-1 bzr1-2*. Asterisks represent premature stop codons.

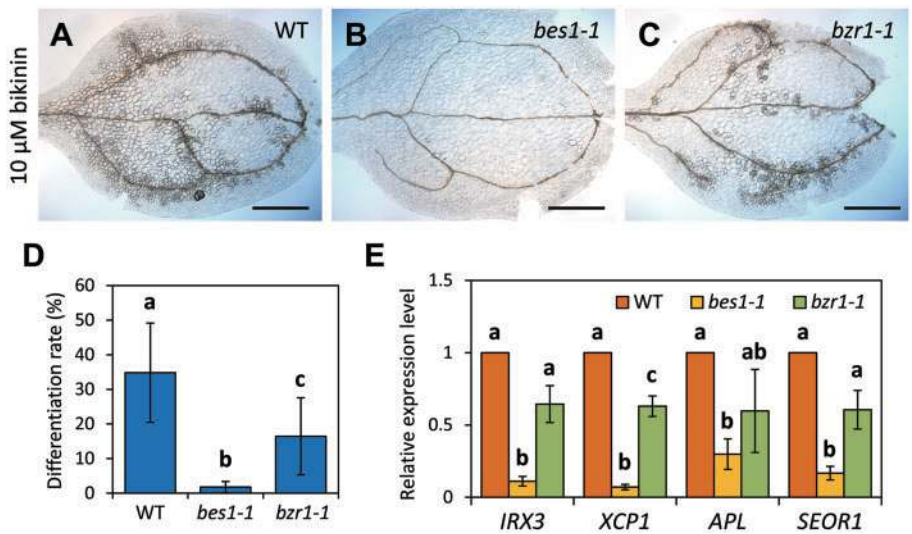

Fig. 5 Mutant phenotypes of *bzr1-1* in VISUAL. (A–C) Ectopic xylem cell formation in VISUAL. WT (A), *bes1-1* (B) and *bzr1-1* (C) cotyledons were cultured for 4 d. Scale bars indicate 1 mm. (D) Quantification of xylem differentiation rates in (A–C). Error bars indicate the SD (n = 8). Significant differences are indicated by different letters (Tamhane T2 test, α = 0.05). (E) Expression levels of xylem and phloem marker genes in the WT, *bes1-1* and *bzr1-1* in VISUAL. RNA was extracted from cotyledons at 72 h after VISUAL induction. Relative expression levels were calculated by comparison with the WT. Error bars indicate the SD (n = 3). Significant differences are indicated by different letters (Tamhane T2 test, α = 0.05).

BZR1 is also a positive regulator of xylem and phloem differentiation from procambial cells

Although we did not detect mutant vascular phenotypes in *bzr1* in planta, the VISUAL system could visualize them. VISUAL using *bzr1-1* and *bes1-1 bzr1-2* revealed that BZR1 as well as BES1 positively regulates both xylem and phloem differentiation from procambial cells. This finding is consistent with the previous finding that both *bes1-D* and *bzr1-D* can partially rescue the phenotype of the *octopus* mutant, in which root protophloem differentiation is prone to be repressed (Anne et al. 2015). Our observation that phloem cells are ectopically produced in hypocotyls of *bes1-D bzr1-D* also supports the molecular functions of BES1 and BZR1 found in VISUAL. In the current study, *bes1* exhibited a

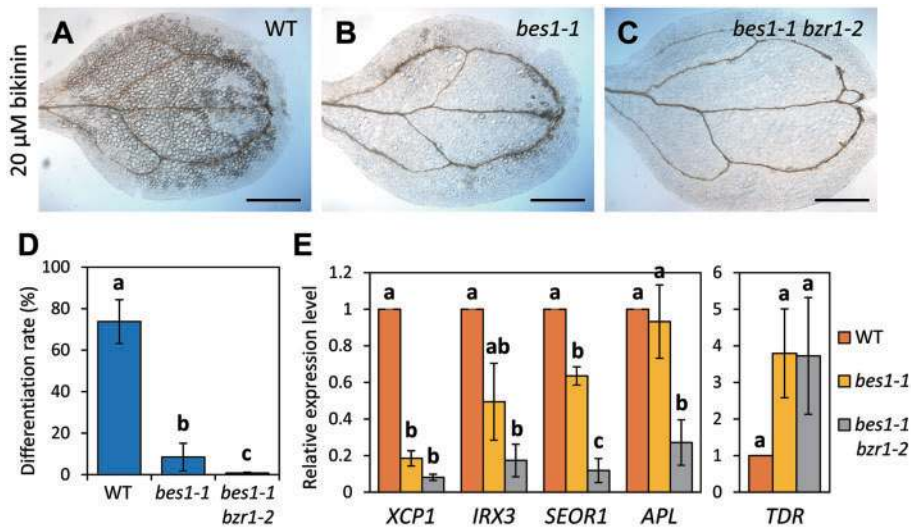

Fig. 6 Mutant phenotypes of *bes1-1 bzr1-2* in VISUAL. (A–C) Ectopic xylem cell formation in VISUAL. WT (A), *bes1-1* (B) and *bes1-1 bzr1-2* (C) cotyledons were cultured with bikinin at twice the normal concentration (20 μM) for 4 d. Scale bars indicate 1 mm. (D) Quantification of xylem differentiation rates in (A–C). Error bars indicate the SD (n = 8–12). Significant differences are indicated by different letters (Tamhane T2 test, α = 0.05). (E) Expression levels of xylem, phloem and procambium marker genes in the WT, *bes1-1* and *bes1-1 bzr1-2* in VISUAL in the presence of 20 μM bikinin. RNA was extracted from cotyledons at 72 h after induction. Relative expression levels were calculated by comparison with the WT. Error bars indicate the SD (n = 3). Significant differences are indicated by different letters (Tamhane T2 test, α = 0.05).

stronger vascular phenotype than *bzr1-1*, and the phenotype induced by these mutations was additive, suggesting that BES1 and BZR1 redundantly function in xylem and phloem differentiation to a greater and lesser extent, respectively. This result is also in accordance with the finding that *bes1-D*, but not *bzr1-D*, shows defects in the hypocotyl vasculature (Kondo et al. 2014).

In VISUAL, mesophyll cells initially differentiate into procambial cells, followed by xylem or phloem cells (Kondo et al. 2015, Kondo et al. 2016). Bikinin promotes procambial cell differentiation (Kondo et al. 2015) as well as the differentiation of procambial cells into xylem and phloem cells (Kondo et al. 2016). However, BES1 and BZR1 only regulate differentiation into xylem and phloem cells. Therefore, it is likely that GSK3s also control procambial cell differentiation, but factors other than BES1 and BZR1 are involved in this process downstream of the GSK3s. Indeed, GSK3s phosphorylate various developmental regulators such as ENHANCER OF GLABRA 3 (EGL3) and TRANSPARENT TESTA GLABRA 1 (TTG1) (Cheng et al. 2014) for root hair formation and AUXIN RESPONSE FACTOR 7 (ARF7) and ARF19 for lateral root formation (Cho et al. 2014). Therefore, it will be interesting to identify a new target(s) of GSK3s that regulates procambial cell differentiation.

Materials and Methods

Plant materials

Seeds of the *Arabidopsis thaliana* *bes1-1* (SALK_098634), *bes1-2* (WiscDsLox246D02) and *bes1-3* (SALK_091133) mutants were obtained from the ABRC stock center. The progeny of heterozygous *bri1-48* (SALK_041648) were gifts from Dr. Takeshi Nakano, and homozygous mutants were identified based on the presence of severely shortened hypocotyls. *bes1-D* and *bzr1-D* mutants were also gifts from Dr. Takeshi Nakano, and *bes1-D bzr1-D* mutants were generated by crossing. All mutants in this study were in the Col-0 background. To produce the complementation lines, DNA fragments of *gBES1* containing the 2,000 bp promoter sequence and the 1,000 bp sequence downstream of the stop codon were cloned and introduced into the pGWB1 vector (Nakagawa et al. 2007), followed by transformation into *bes1-1* by the floral dip method (Clough and Bent 1998). Plants were grown on conventional 1/2 MS agar plates (pH 5.7) at 22°C under continuous light unless otherwise mentioned. For later harvesting, seedlings were transferred to pots containing a mixture of vermiculite (VS Kakou) and PRO-MIX BX (Premier Horticulture).

CRISPR

The target sequence was selected using CRISPRdirect software (Naito et al. 2015). DNA fragments containing 20 bp of the target sequence neighboring the PAM (protospacer adjacent motif) sequence and overhang sequences were generated by hybridizing two primers, followed by ligation into the pEn-Chimera vector (Fauser et al. 2014) that had been digested with *Bbs*I. The single guide RNA (sgRNA)-containing sequence was then transferred into the pDe-CAS9 vector (Fauser et al. 2014) via LR reaction (Thermo Fisher Scientific). The resulting construct was transformed into WT and *bes1-1* plants. Transformants were obtained by bialaphos selection. T_2 seeds from single insertion lines were incubated on MS agar plates without antibiotics. *Cas9*-free mutants were selected from the T_2 population by PCR and sequencing using the primers listed in **Supplementary Table S2**. To check the sequence of the *BZR1* transcript in *bes1-1 bzr1-2*, total RNA was extracted from cotyledons of 6-day-old WT and *bes1-1 bzr1-2* plants using an RNeasy Plant Mini kit (Qiagen). Reverse transcription was performed using SuperScript III (Thermo Fisher Scientific). PCR was performed using synthesized cDNA and the primers listed in **Supplementary Table S2**, followed by sequencing using the same primer. Data were visualized using Chromas 2.6 (http://technelysium.com.au/wp/).

VISUAL

The detailed protocol for VISUAL was described previously (Kondo et al. 2016). In brief, cotyledons of 6-day-old seedlings grown in liquid 1/2 MS medium were

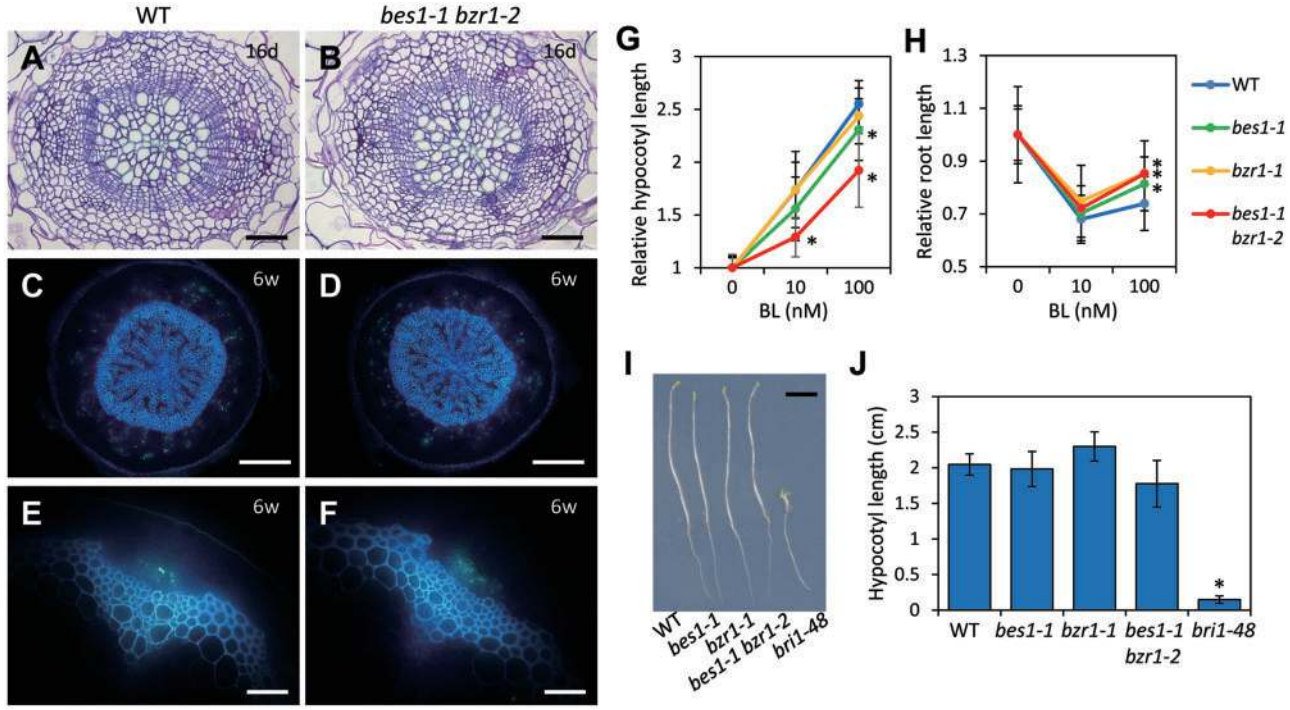

Fig. 7 In vivo phenotype of *bes1-1 bzr1-2*. (A–F) Cross-sections of hypocotyls (A–D) and stems (E, F) of WT (A, C, E) and *bes1-1 bzr1-2* (B, D, F) plants grown for 16 d (A, B) or 6 weeks (C–F). Toluidine blue (A, B) or aniline blue staining (C–F) was conducted. Blue and green fluorescence in (C–F) is autofluorescence from xylem cells and stained phloem cells after UV radiation, respectively. Scale bars indicate 200 μm for (C) and (D) and 50 μm for the others. (G, H) BL sensitivity of WT, *bes1-1*, *bzr1-1* and *bes1-1 bzr1-2* seedlings. Relative lengths of hypocotyls (G) and roots (H) were calculated by comparison with samples of each genotype grown without BL. Error bars indicate the SD (n = 30–32 except for n = 25 for *bzr1-1* treated with 10 nM BL). (I) Hypocotyl elongation in plants grown in the dark. Seedlings were grown for 7 d. The scale bar indicates 0.5 cm. (J) Quantification of hypocotyl elongation in (I). Error bars indicate the SD (n = 3–6). Significant differences compared with the WT were examined by Tamhane T2 test (α = 0.05).

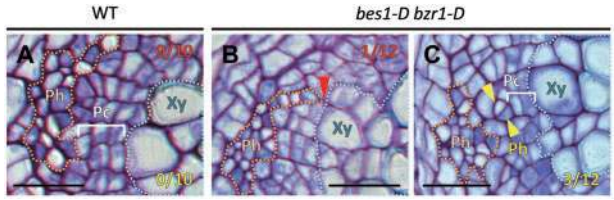

Fig. 8 Comparison of hypocotyl vasculature between WT and *bes1-D bzr1-D*. Cross-sections of hypocotyls of WT (A) and *bes1-D bzr1-D* (B, C) plants grown for 11 d. Orange and blue dotted lines indicate phloem (Ph) and xylem (Xy) cells, respectively. White solid lines indicate procambial cell (Pc) layers. Red and yellow arrowheads indicate the adjacency of xylem and phloem cells and non-clustered phloem cells, respectively. The fraction in the top and bottom of the panels represents the number of plants exhibiting adjacency of xylem and phloem cells and non-clustered phloem cells per total number of plants observed, respectively. Scale bars indicate 20 μm.

cultured in MS-based medium containing 0.25 mg l^{-1} 2,4-D, 1.25 mg l^{-1} kinetin and 10 μM bikinin under continuous light. To compare the phenotypes of *bes1-1* vs. *bes1-1 bzr1-2*, the bikinin concentration was changed to 20 μM. To observe ectopic xylem differentiation, cotyledons cultured for 4 d were fixed in ethanol/acetic acid (3 : 1) and mounted with clearing solution (chloral hydrate/glycerol/water; 8 : 1 : 2). The differentiation rates were determined based on the area of ectopic xylem cells in a cotyledon per total area of the cotyledon blade. These areas were calculated using ImageJ.

qRT-PCR

Total RNA was extracted from cotyledons before or after culture for 72 h (in the VISUAL experiments) or from whole seedlings treated with dimethylsulfoxide (DMSO) or 100 μM BL for 3 h (in the BL sensitivity tests) using an RNeasy Plant Mini kit (Qiagen). Quantitative PCR was performed using a LightCycler (Roche Diagnostics). *UBIQUITIN 14* (*UBQ14*) was used for the VISUAL experiments, and *ACTIN 2* (*ACT2*) was used for the BL sensitivity tests as an internal control. The gene-specific primer sets are listed in **Supplementary Table S2**.

Microarray experiment

Microarray analyses were performed as previously described (Ohashi-Ito et al. 2010). For clustering, normalization of gene expression levels was performed as follows: first, the average fold change between values before and after induction in each experiment was calculated. These values were then normalized by dividing them by the median value of the WT, *bes1-3* and *bes1-1*. Finally, these values were converted to the $\log_2$ scale, producing a value defined as the Processed signal. Hierarchical clustering via the Pearson correlation method and heatmap generation were performed using Subio Platform software (Subio). The half-time point was defined as the first time point when the relative expression level reached 50% of its maximum value in a set of time course microarray data (Kondo et al. 2015) in which the expression levels between observed values were postulated to change linearly. GO enrichment analysis was performed using DAVID Bioinformatics Resources 6.8 (Huang et al. 2009; https://david.ncifcrf.gov/).

Histological analysis

Cross-sections of hypocotyls of 11- or 16-day-old plants grown in liquid 1/2 MS medium were produced as previously described (Kondo et al. 2014). Sliced samples were stained with 0.1% toluidine blue for 1 min. To produce cross-

sections of 6-week-old plants, hypocotyls or the basal parts of stems were fixed in 70% ethanol. Sections of hypocotyls and stems 2 cm above the rosette at 80 μm thickness were produced using a LEICA VT1200S vibratome. Sliced samples were stained with 0.05% aniline blue in 100 mM phosphate buffer (pH 7.2) for 1 h and observed under UV radiation.

BR treatment

To observe hypocotyl or root elongation, plants were grown on 1/2 MS agar plates containing DMSO or BL. After 7 d, the plates were scanned with a CanoScan 9000F (Canon). Hypocotyl and root lengths were measured using ImageJ. For gene expression analysis, plants were grown on 1/2 MS agar plates. After 10 d, the seedlings were incubated in a solution of DMSO or 100 μM BL for 3 h and collected for RNA extraction.

Phenotypic observation of dark-grown plants

Plants were grown on 1/2 MS agar plates in the dark after white light irradiation to promote germination. After 7 d, the plates were scanned using a CanoScan 9000F (Canon). Hypocotyl length was measured using ImageJ.

Statistical analysis

For multiple comparisons, Tamhane T2 tests were employed in this study due to inhomogeneous variances obtained by the Levene tests (Wallner et al. 2017). The significance thresholds were set to $\alpha = 0.05$. The *P*-values for each comparison were calculated by Welch's *t*-test. The significance threshold of each comparison was set to $\alpha' = 1 - (1 - \alpha)^{1/k}$, where k is the total number of comparisons. For example, if $k = 3$, the significance threshold of the *P*-value of each comparison (α') is approximately 0.0167.

Supplementary Data

Supplementary data are available at PCP online.

Funding

This work was supported by the Ministry of Education, Culture, Sports, Science and Technology of Japan [Grants-in-Aid No. 17H06476 to Y.K. and No. 15H05958 to H.F.] and the Japan Society for the Promotion of Science [grant No. 16J06222 to M.S., No. 17H05008 to Y.K. and No. 16H06377 to H.F.].

Acknowledgments

We thank Yukiko Sugisawa, Yasuko Ozawa and Satoshi Endo for technical support. We also thank Holger Puchta and Takeshi Nakano for providing materials.

Disclosures

The authors have no conflicts of interest to declare.

References

Anne, P., Azzopardi, M., Gissot, L., Beaubiat, S., Hématy, K. and Palauqui, J.C. (2015) OCTOPUS negatively regulates BIN2 to control phloem differentiation in Arabidopsis thaliana. *Curr. Biol.* 25: 2584–2590.

Bonke, M., Thitamadee, S., Mähönen, A.P., Hauser, M.T. and Helariutta, Y. (2003) APL regulates vascular tissue identity in *Arabidopsis*. *Nature* 426: 181–186.

Cheng, Y., Zhu, W., Chen, Y., Ito, S., Asami, T. and Wang, X. (2014) Brassinosteroids control root epidermal cell fate via direct regulation of a MYB–bHLH–WD40 complex by GSK3-like kinases. *eLife* 3: e02525.

Cho, H., Ryu, H., Rho, S., Hill, K., Smith, S., Audenaert, D., et al. (2014) A secreted peptide acts on BIN2-mediated phosphorylation of ARFs to potentiate auxin response during lateral root development. *Nat. Cell Biol.* 16: 66–76.

Clough, S.J. and Bent, A.F. (1998) Floral dip: a simplified method for *Agrobacterium*-mediated transformation of *Arabidopsis thaliana*. *Plant J.* 16: 735–743.

De Rybel, B., Audenaert, D., Vert, G., Rozhon, W., Mayerhofer, J., Peelman, F., et al. (2009) Chemical inhibition of a subset of *Arabidopsis thaliana* GSK3-like kinases activates brassinosteroid signaling. *Chem. Biol.* 16: 594–604.

Fauser, F., Schiml, S. and Puchta, H. (2014) Both CRISPR/Cas-based nucleases and nickases can be used efficiently for genome engineering in *Arabidopsis thaliana*. *Plant J.* 79: 348–359.

Furuta, K.M., Hellmann, E. and Helariutta, Y. (2014a) Molecular control of cell specification and cell differentiation during procambial development. *Annu. Rev. Plant Biol.* 65: 607–638.

Furuta, K.M., Yadav, S.R., Lehesranta, S., Belevich, I., Miyashima, S., Heo, J.O., et al. (2014b) Arabidopsis NAC45/86 direct sieve element morphogenesis culminating in enucleation. *Science* 345: 933–937.

Guo, H., Li, L., Aluru, M. and Yin, Y. (2013) Mechanisms and networks for brassinosteroid regulated gene expression. *Curr. Opin. Plant Biol.* 16: 545–553.

He, J.X., Gendron, J.M., Sun, Y., Gampala, S.S., Gendron, N., Sun, C.Q., et al. (2005) BZR1 is a transcriptional repressor with dual roles in brassinosteroid homeostasis and growth responses. *Science* 307: 1634–1638.

Huang, D.W., Sherman, B.T. and Lempicki, R.A. (2009) Systematic and integrative analysis of large gene lists using DAVID Bioinformatics Resources. *Nat. Protoc.* 4: 44–57.

Kang, S., Yang, F., Li, L., Chen, H., Chen, S. and Zhang, J. (2015) The Arabidopsis transcription factor BRASSINOSTEROID INSENSITIVE1-ETHYL METHANESULFONATE-SUPPRESSOR1 is a direct substrate of MITOGEN-ACTIVATED PROTEIN KINASE6 and regulates immunity. *Plant Physiol.* 167: 1076–1086.

Kondo, Y., Fujita, T., Sugiyama, M. and Fukuda, H. (2015) A novel system for xylem cell differentiation in *Arabidopsis thaliana*. *Mol. Plant* 8: 612–621.

Kondo, Y., Ito, T., Nakagami, H., Hirakawa, Y., Saito, M., Tamaki, T., et al. (2014) Plant GSK3 proteins regulate xylem cell differentiation downstream of TDIF–TDR signalling. *Nat. Commun.* 5: 3504.

Kondo, Y., Nurani, A.M., Saito, C., Ichihashi, Y., Saito, M., Yamazaki, K., et al. (2016) Vascular Cell Induction Culture System Using Arabidopsis Leaves (VISUAL) reveals the sequential differentiation of sieve element-like cells. *Plant Cell* 28: 1250–1262.

Kubo, M., Udagawa, M., Nishikubo, N., Horiguchi, G., Yamaguchi, M., Ito, J., et al. (2005) Transcription switches for protoxylem and metaxylem vessel formation. *Genes Dev.* 19: 1855–1860.

Lachowiec, J., Lemus, T., Thomas, J.H., Murphy, P.J., Nemhauser, J.L. and Queitsch, C. (2013) The protein chaperone HSP90 can facilitate the divergence of gene duplicates. *Genetics* 193: 1269–1277.

Li, J. and Chory, J. (1997) A putative leucine-rich repeat receptor kinase involved in brassinosteroid signal transduction. *Cell* 90: 929–938.

Li, J. and Nam, K.H. (2002) Regulation of brassinosteroid signaling by a GSK3/SHAGGY-like kinase. *Science* 295: 1299–1301.

Naito, Y., Hino, K., Bono, H. and Ui-Tei, K. (2015) CRISPRdirect: software for designing CRISPR/Cas guide RNA with reduced off-target sites. *Bioinformatics* 31: 1120–1123.

Nakagawa, T., Kurose, T., Hino, T., Tanaka, K., Kawamukai, M., Niwa, Y., et al. (2007) Development of series of gateway binary vectors, pGWBs, for realizing efficient construction of fusion genes for plant transformation. *J. Biosci. Bioeng.* 104: 34–41.

Ohashi-Ito, K., Oda, Y. and Fukuda, H. (2010) *Arabidopsis* VASCULAR-RELATED NAC-DOMAIN6 directly regulates the genes that govern

programmed cell death and secondary wall formation during xylem differentiation. *Plant Cell* 22: 3461–3473.

Wallner, E.S., López-Salmerón, V., Belevich, I., Poschet, G., Jung, I. and Grünwald, K., et al. (2017) Strigolactone- and karrikin-independent SMXL proteins are central regulators of phloem formation. *Curr. Biol.* 27: 1241–1247.

Wang, Y., Sun, S., Zhu, W., Jia, K., Yang, H. and Wang, X. (2013) Strigolactone/MAX2-induced degradation of brassinosteroid transcriptional effector BES1 regulates shoot branching. *Dev. Cell* 27: 681–688.

Wang, Z.Y., Nakano, T., Gendron, J., He, J., Chen, M., Vafeados, D., et al. (2002) Nuclear-localized BZR1 mediates brassinosteroid-induced growth and feedback suppression of brassinosteroid biosynthesis. *Dev. Cell* 2: 505–513.

Yamaguchi, M., Mitsuda, N., Ohtani, M., Ohme-Takagi, M., Kato, K. and Demura, T. (2011) VASCULAR-RELATED NAC-DOMAIN7 directly regulates the expression of a broad range of genes for xylem vessel formation. *Plant J.* 66: 579–590.

Yin, Y., Vafeados, D., Tao, Y., Yoshida, S., Asami, T. and Chory, J. (2005) A new class of transcription factors mediates brassinosteroid-regulated gene expression in *Arabidopsis*. *Cell* 120: 249–259.

Yin, Y., Wang, Z.Y., Mora-Garcia, S., Li, J., Yoshida, S., Asami, T., et al. (2002) BES1 accumulates in the nucleus in response to brassinosteroids to regulate gene expression and promote stem elongation. *Cell* 109: 181–191.

Yokoyama, A., Yamashino, T., Amano, Y., Tajima, Y., Imamura, A., Sakakibara, H., et al. (2007) Type-B ARR transcription factors, ARR10 and ARR12, are implicated in cytokinin-mediated regulation of protoxylem differentiation in roots of *Arabidopsis thaliana*. *Plant Cell Physiol.* 48: 84–96.